Flexible Model-based Multi-corner Detector for Accurate Measurements and Recognition

Gustavo Olague

Departamento de Ciencias de la Computación
Centro de Investigación Científica y de Educación
Superior de Ensenada, Km 107 Carretera
Tijuana-Ensenada, 22860, Ensenada,B.C., México
olague@cicese.mx

Benjamin Hernández

Instituto de Astronomía, Ensenada
Universidad Nacional Autónoma de México
Observatorio Astronómico Nacional
Km 103 Carr. Tijuana-Ensenada, 22830 Ensenada.
benja@astrosen.unam.mx

Abstract

Recognition and photogrammetric tasks require models capable of detecting and measuring complex features normally found in all kind of natural and artificial scenes. Corners are special features in images, and are of great use in computing camera calibration, tracking and reconstruction. Basically, a corner is defined as the junction point of two or more straight-line edges. Previous methods devoted to corner detection are based on parametric models. However, a drawback from previous approaches is the cumbersome of the proposed models. This paper presents a new multi-corner detector based on a unit step edge function (USEF) that defines a straight line edge. Several USEFs are combined to produce complex corners using simple operators as addition and multiplication. As well as previous methods we search model parameters characterizing completely single gray-value structures by means of least squares fit of the model to the observed image intensities. Examples and experimental results illustrate the quality and efficacy of the detectors.

1. Introduction

Computer vision relies on image processing techniques in order to obtain the information required for tasks devoted to perceiving, sensing and measuring the world around a machine vision system. Most gray scale corner detectors assume an idealized corner that is sharply pointed and has straight, steep edges and return just a single value measuring the "cornerity" or "strenght" of the corner (e.g. [3, 4, 8, 12]). However, corners rarely appear like this in the real world. Due to manufacturing limitations, wear and tear, streamlining, aesthetics, and so forth, corners are more tipically rounded, blunted, blurred, ragged, textured, etc. Rosin [11] lists these attributes in more detail. In particular, cornerity presents the following properties: Position or location, angle of aperture, orientation, edge shape, edge texture, contrast, edge profile, sharpness, color, junction type and size. This paper presents a novel multi-corner image model based on straight lines that are merged using simple operators like addition and multiplication. Our corner detector is a parametric based model detector, which provides with most of the above properties. The problem of L-corner detection is explained extensively in this paper. The displacement of the L-corner must be approched carefully in the case of a bandlimited system. This problem is of main concern for high accurate reconstruction. In this contribution we will use the concept that corners are always a subset of edges instead of adjacent surfaces. Surely, if three or more surfaces meet then there always be a corner. However, when two surfaces meet it is not clear whether is just a normal edge or an L-corner.

1.1. Previous Work

Our review is not intended to be exhaustive nor does it aim to present corner detectors in detail. An approach for detecting edges is the use of the Laplacian-of-Gaussian (LoG) [7]. It is widely accepted that the position of the L-corner is extracted exactly and independently of the amount of blur. As we will see in the paper we question this belief. As a result we will propose a new corner criterion for accurate measurement. An approach combining the properties of direct corner detectors and the localization behavior of the LoG for L-junctions can be found in Deriche and Giraudon [4]. Their approaches relies on local maxima of the determinant of the Hessian matrix, which are tracked across different image scales. One problem is that for a trihedral corner the number of local maxima depends on the

1051-4651/02 $17.00 © 2002 IEEE

heights of the different intensity plateaus. For more complex corners the constellations and therefore the tracking of local maxima in scale space will become even more difficult. Parametric feature detectors [1] aim at matching a multi-parameter model to a digital image. These detectors work directly on the grey-level image. Most of them aimed at detecting the corners within subpixel resolution. The appearance of such a feature in an image may well depend upon a number of parameters such as orientation, localization, scale and level of blurring. Rhor [10] studied the displacement of the location using an analytical model of the corners, which introduces a smoothing procedure given by a Gaussian function that convolves with the corner model. The objective of this work is to develop an algorithm that automatically constructs a feature detector for an arbitrary parametric feature. We concentrate our study here on L-corners and how the corner position is displaced for purpose of photogrammetric measurement. The approach can easily be extended to complex features for purpose of object recognition. Nevertheless, the displacement of complex features are more difficult to obtain due to the geometric reasoning used.

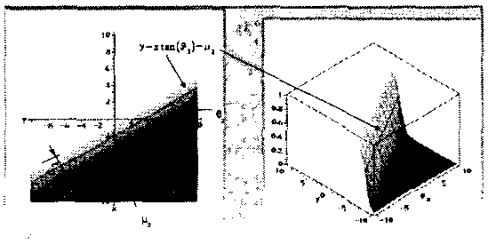

Figure 1. *These figures show the straight line and its equation together with the unit step edge function $U_y(I,P)$.*

2 Unit Step Edge Function Model

Let the image coordinates and the set of unknown model parameters be denoted by $I=(x,y)$ and $P=(p_1,\ldots,p_n)$ respectively. The unit step edge function is represented as follows:

$$U_x(I,P_x)=\pm\frac{1}{\sigma_1\sqrt{2\pi}}\int e^{\frac{-(x-y\cdot\tan(\theta_1)-\mu_1)^2}{2\sigma_1^2}}dx+\frac{1}{2} \quad (1)$$

where the image coordinates range from $[-W,W]$. The central point μ_1 designs the position x of the line that crosses along the y-axis. μ_1 ranges from $[-W,W]$. The rotation θ_1 is made clockwise about the (positive) y-axis. θ_1 designs the orientation of the edge model to be fitted to the image within the range $-\frac{\pi}{2}\leq\theta_1\leq\frac{\pi}{2}$. Finally a scaling factor σ_1 that characterizes the amount of blur introduced by the discretization process needs to be taken into account. σ_1 ranges from $[0,W]$. The unit edge function describes a probability density function that increases steadily from 0 to 1 with respect to the x-axis. Its graph is the three-dimensional step edge shown in figure 1. This model describes completely the 2D intensity variations within a single equation instead of the two step process of convolving an ideal shaped grey value structure with a Gaussian filter as is normally used. In this way, it is straightforward to scale the model to the 2D intensity variations using the operations of addition and multiplication as follows:

$$U_x(I,P_x')=U_x(I,P_x)A+B \quad (2)$$

where A represents the distance between the lower and upper grey levels and B represents the lower grey value also called here floor level. The unit step edge function $U_y(I,P_y)$ with respect to the y-axis is represented in a similar way where all intervals of the variables remain the same: μ_2 designs the position y of the line that crosses along the x-axis. The rotation θ_2 designs the orientation of the unit step edge model in the y direction. $U_y(I,P_y)$ can be evaluated numerically using the Gaussian error function as follows:

$$U_y(I,P_y)=\pm\frac{1}{2}erf\left(\frac{\sqrt{2}(-y+x\cdot\tan(\theta_1)+\mu_2)}{2\sigma_2}\right)+\frac{1}{2} \quad (3)$$

Hence USEF is characterized by a r_2 straight line along its main direction. The straight line equation is obtained from the numerator on the exponent of the exponential function, see Figure 1.

3 L-corner Unit Function

This paper presents a new Corner Unit Function (CUF) that is based on two USEF. We combine both USEF as follows, see Figure 2:

$$C(I,P)=U_x(I,P_x)\cdot U_y(I,P_y) \quad (4)$$

Therefore, in order to obtain the corner model we simply multiply both USEF. In summary our model is based on an analytical expression with the following characteristics:

1. Each edge on the corner has different levels of blurring. This is physically produced by a non-square pixel CCD camera as the Pulnix 9701. Hence, the CUF models the degree of blurring for each edge.

2. Each angle is independent. Therefore, we do not have any restrictions with respect to the acute or obtuse of the corner.

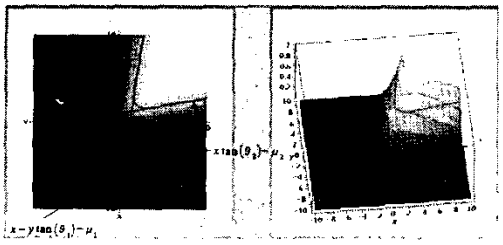

Figure 2. *These figures show both straight lines and their equations together with the corner unit function $C(I,P)$.*

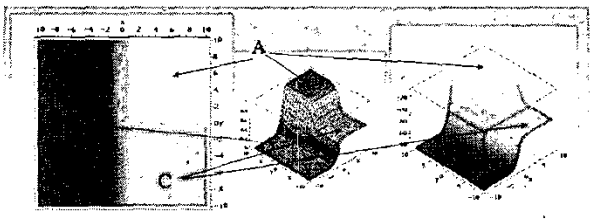

Figure 3. *The vertex model can be easily obtained from an L-corner model and the USEF.*

3. The corner moves freely around the explored window. We obtain the position and orientation of the corner around any point within the studied window.
4. The grey levels are self-adjusted inside and outside of the corner.

This kind of corner is called L-corner in the literature.

4 Extraction of Multiple Features

Following the same procedure of using Equation 1 we can model arbitrary complex grey value structures in terms of step edge functions by means of simple addition and multiplication operations. The total number of parameters used by the model is in general:

$$n = 3 + 2N + O \tag{5}$$

where the first three, in the case of the L-corner, are given by the amount of blur σ and the lower and upper grey values A and B respectively. N represents the number of step edge models and O specifies the number of operations used to represent the feature. In fact the first three should be increased if we take into account different blurs for each main direction and multiple grey values when considering more complex models as shown in figure 3. A vertex model (VUF) can be easily obtained from an L-corner model (CUF) and the USEF. The vertex model needs an extra grey level and in total we need 12 parameters to model the corner.

$$V(I,P) = U_x(I,P_x)\cdot U_y(I,P_y)\cdot A + U_z(I,P_{x*})\cdot B + C \tag{6}$$

5 Displacement of the L-corner

For fitting the general model to intensity variations we need to compute the partial derivatives through the evaluation of analytical expressions. This task is achieved relatively simple through the use of Maple. Having defined the general parametric model to intensity variations we need to evaluate the displacement of the L-corner point considering the blurring effects along each main direction. The straight line that characterizes the USEF is given by $x - y\cdot\tan(\theta_1) - \mu_1$ along the x-axis, and by $y - x\cdot\tan(\theta_2) - \mu_2$ along the y-axis. These two equations are obtained from the numerator on the exponent of the exponential function. The point of intersection (x_0, y_0) of both equations is given as follows:

$$\left(X_0 = \frac{\tan(\theta_1)\mu_2 + \mu_1}{-1 + \tan(\theta_2)\tan(\theta_1)}, Y_0 = \frac{\tan(\theta_2)\mu_1 + \mu_2}{-1 + \tan(\theta_2)\tan(\theta_1)}\right) \tag{7}$$

Each straight line is asymptotic to the contour level $C(I,P) = 0.5$ as is shown in Figure 4. Each straight line

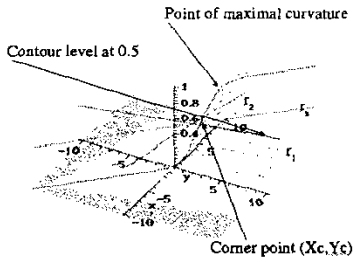

Figure 4. *This figure shows the exact position of the L-corner point we are searching for along the r_s straight line that is changing its orientation between the r_1 and r_2 straight lines.*

can be seen as defining a vector. Using both vectors and the scalar or inner product we can calculate the angle between both straight lines. Our goal is to find the corner point (X_c, Y_c). Since our problem is defined geometrically we can define a line that cross the intersection point and lies between the two lines that characterizes the L-corner. The corner should be at the point where $C(I,P) = 0.5$. We can now (numerically) calculate the position that satisfies the above implicit equation using the algorithms of bracketing

and bisection. However, we still need to find the best point along the implicit curve that defines the exact place for the L-corner. In order to solve this problem, we use the downhill simplex method for searching the point that minimizes the Euclidean distance $D_{\min}$ between the intersection point and the corner point. The exact corner point will be then the point that minimizes the distance $D_{\min}$ and satisfies the implicit equation $C(I,P) = 0.5$. Traditionally the position of the L-corner point that is search for by direct corner detectors and indirect approaches was defined as the point of maximum curvature of linked edge points and that just one blur factor was considered in the analysis. Deriche reports that the corner is found at the point where the Laplacian is zero. Figure 4 is a three-dimensional representation of our model that exemplifies graphically our criteria for localizing the exact position of the L-corner point. It is evident that the point of maximum curvature has a symmetric point localized at the lower part of the corner. Considering this fact we propose by geometry that the middle point along the curve that goes from top to bottom satisfies in an optimal manner the exact position of the L-corner point. Our modeling takes into account that a corner can be displaced due to different blurs produced by the shape and size of the photosensitive elements within a CCD image sensor. Because each USEF is independent of each other there are any restrictions about the acute or obtuse of the angle between both straight lines. Moreover, the L-corner can be moved around the complete window being explored.

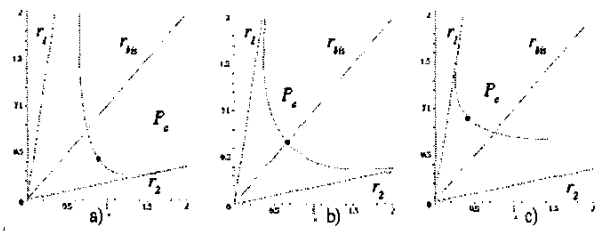

Figure 5. *Curve distortion using several blur factors: a)$\sigma_1 = 0.5, \sigma_2 = 4$, b)$\sigma_1 = \sigma_2 = 1.0$, c)$\sigma_1 = 4, \sigma_2 = 0.5$.*

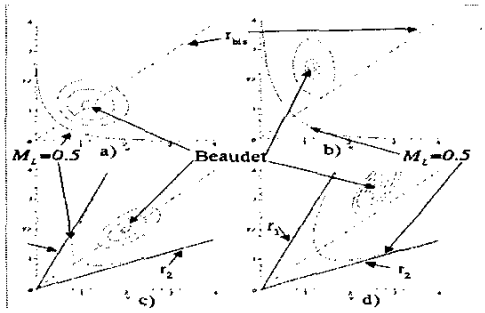

Figure 6. *Exact Beaudet corner position using several blur factors and angles of aperture.*

6 Comparing CUF Model with Previous L-corner detectors

Last section introduces our criteria for extracting the exact corner position. Figure 5, shows the behaviour of corner location with respect to the blur factor. Clearly, the corner is displaced with respect to the bisector line when both factors are different. Our goal here is to show how the criteria for corner location used by Beaudet[2], Dreschler and Nagel[5], Kitchen and Rosenfeld[6], Deriche and Giraudon[4] and Rohr[10] are different and similar to the criteria proposed in this paper. As a result, we expect to give confidence on the usefulness of our approach.

The first three detectors proposed for comparison were developed for pixel resolution. However, the criteria can be applied to our L-corner model for purpose of contrasting the similarities and differences. Beaudet[2] proposed a rotationally invariant operator based on the determinant of the Hessian associated to the image. Figure 6, shows the behaviour of the detector for four sets of parameters. As a result, we observe that the corner location is displaced towards the top of the corner. Using the same blur factor the maximum is found along the bisector line r_{bis}. Considering different blur factors the corner is found between r_{bis} and r_1. However, our criteria is found between r_{bis} and r_2 with a less important displacement. Hence, we can consider the detector proposed by Beaudet as unstable with respect to the angle of aperture and blurring factors. Dreschler and Nagel[5] proposed an operator based on Gaussian curvature principle. In order to locate the corner, two points (maximum and minimum) are first located, then the point between both points where the principal curvature crosses zero is designed as the corner. Figure 7, shows the behaviour of the corner detector. As well as Beaudet detector, Dreschler and Nagel corner detector suffer of the same undesirable characteristics. Kitchen and Rosenfeld[6] proposed a measure of cornerness based on an operator that corresponds at the curvature scaled by the gradient magnitude. Figure 8, shows the behaviour of the operator with respect to the contour curve $C(I,P) = 0.5$, the aperture angle, as well as for some different blur factors. As a result, we observe that the corner location is displaced towards the top of the corner. Using the same blur factor the corner is found along the bisector line. Considering different blur factors the corner is found between r_{bis} and r_2. Hence, Kitchen and Rosenfeld detector agrees well with respect to our criteria for corner location. However, it is still different from the point of view of displacement.

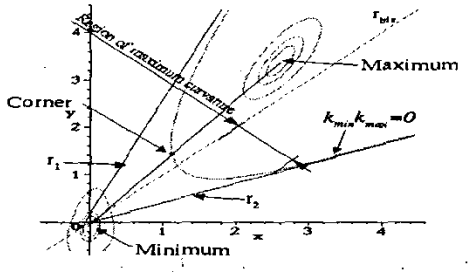

Figure 7. *Exact Dreschler and Nagel corner position using an angle of aperture of* $45°$ *and blur factors of* $\sigma_1 = 1$ *and* $\sigma_2 = 2$.

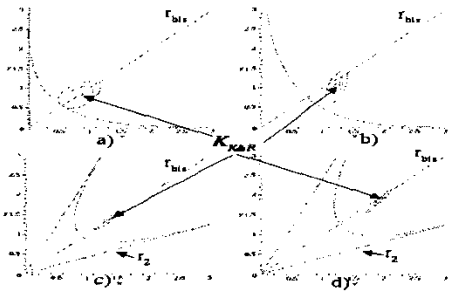

Figure 8. *Exact Kitchen and Rosenfeld corner position using several angles of aperture and blur factors.*

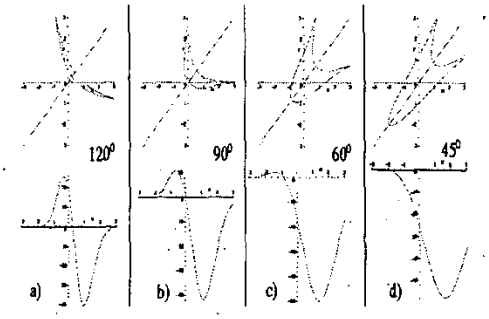

Figure 9. *Zero crossing behaviour of the Laplacian using different angles of aperture.*

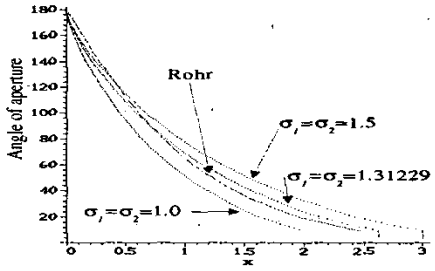

Figure 10. *Displacement of Rohr corner position with respect to the angle of aperture as well as our model using several blur factors.*

Deriche and Giraudon[4] study analytically the behaviour of corners in the scale space. They proposed an approach in order to correct the displacement of corner position as follows: First a Laplacian image is calculated. Second, Beaudet's measure at two scales are calculated and an extrema detection in all directions is performed. Around each detected extrema in the image corresponding to the first scale, we look in the second image for the position of the local maxima. Once this second maxima detected, we look for the exact position of the corner as the point that belongs to the line segments joining the two positions and where a zero crossing occurs in the Laplacian image. Figure 9, shows the behaviour of the proposed algorithm. As a result, we observe that the line joining both extrema is the bisector line r_{bis}. The corner location is displaced along the the bisector line at zero-crossing with respect to the angle of aperture. In summary, the approach proposed by Deriche and Giraudon define the location of the corner biased towards the corner floor and the behaviour in general is contrary to the approach proposed in this paper. Finally, Rohr's detector is analyzed using an implicit equation as we made here in a similar way. The position of the corner point is independent of the height between the floor and the top of the corner. There is a linear relationship between the blur factor and the exact position of the corner point. All above considerations agree and are observed in the behaviour of our criteria for corner detection. Figure 10, shows the displacement of position x with respect to the angle of aperture considering Rohr criteria and our criteria using several blur factors. In general, using angles bigger than $90°$ our criteria provides a smaller displacement and for angles smaller than $90°$ occurs the opposite.

As a conclusion, Beaudet, Dreschler and Nagel, and Kitchen and Rosenfeld detectors located the exact position of the corner towards the top of the corner. Deriche and Giraudon located the exact position of the corner point biased towards the floor of the corner. The displacement is contrary to our criteria $C(I, P) = 0.5$ considering the angle of aperture. On the other side, the curve of displacement of the corner point along the x-axis of our model and that pro-

Blurring	σ_1	μ_1	θ_1	A	X_c	Y_c
0.0	0.876	-0.968	1.00	153.6	410.43	198.59
0.05	0.876	-0.968	1.00	153.6	410.43	198.59
0.25	0.876	-0.968	1.00	153.8	410.43	198.59
0.50	0.992	-0.962	0.964	162.3	410.52	198.52
0.75	1.15	-1.00	1.11	165.5	410.58	198.35
1.00	1.19	-1.06	1.19	166.04	410.54	198.22
1.25	1.19	-1.10	1.216	165.96	410.49	198.12

Table 1. Results of our L-corner detector after applying different levels of blurring. We show only the values for the first USEF, the top grey level, as well as the position of the L-corner.

posed by Rohr presents a similar behaviour. Both criteria are similar in behaviour but their deduction raise from very different concepts: our criteria is based on a purely geometric reasoning while the criteria proposed by Rohr employs concepts from differential geometry. The last two detectors were studied here considering equal blur factors along the two main directions for purpose of comparison. However, our model can use different blurs as can arise in the case of a rectangular CCD.

7 Experiments

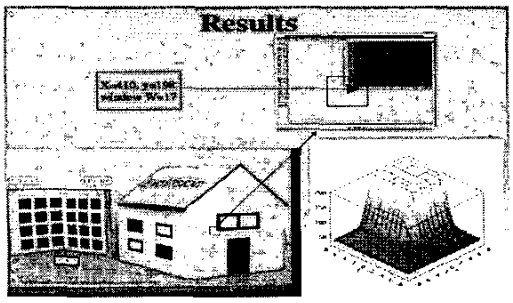

Figure 11. *A zoom of one L-corner of our EvoVision house is shown as well as its final three-dimensional model.*

We have made a series of experiments to test the quality and efficiency of the detector. We present one example of our L-corner detector. Figure 11 shows the calibration grid we have used, as well as a zoom on one of the L-corners and the final result. To test the quality and robustness of our L-corner detector, we applied noise to our test image using a bidimensional Gaussian filter. The results are presented in Table 1. As we can observe the X_c position of the L-corner is very stable. We see that the more we smooth a difference on the Y_c value is more pronounced. This is due to the non-squared pixels of the Pulnix 9701 digital camera. A second test was performed using the well known property of invariance of the cross-ratio and error propagation for obtaining the accuracy of the detector [9]. Final result lets us to affirm that the accuracy is up to 0.01 of a pixel.

8. Summary and Conclusions

The USEF has proved its value for modeling complex corners. Real tests have proved the quality of the L-corner detector up to subpixel accuracy. The flexibility and simplicity of the model are its main characteristics to be explored, for cases even more complex, in the near future.

Acknowledgments

This research was funded by contract 35267-A from CONACyT México.

References

[1] S. Baker, S. K. Nayar and H. Murase. "Parametric Feature Detection". *International Journal of Computer Vision*, 27(1), pp. 27-50, Kluwer Academic Publishers, 1998.

[2] P.R. Beaudet. "Rotational Invariant Image Operators". *International Conference on Pattern Recognition*, pp.579-583, 1978.

[3] R. Deriche. "Using Canny's Criteria to Derive a Recursively Implemented Optimal Edge Detector". *International Journal of Computer Vision*. pp. 167-187, 1987.

[4] R. Deriche and G. Giraudon. "A Computational Approach for Corner and Vertex Detection". *International Journal of Computer Vision*, 10(2), pp. 101-124, Kluwer Academic Publishers, 1993.

[5] L. Dreschler and H.H. Nagel. "On the Selection of Critical Points and Local Curvature Extrema of Region Boundaries for Interframe Matching". *International Conference on Pattern Recognition*, pp. 542-544, 1982

[6] L. Kitchen and A. Rosenfeld. "Gray-Level Corner Detection". *Pattern Recognition Letters*, pp. 95-102, December 1982.

[7] D. Marr and E. Hildreth. "Theory of Edge Detection". *Proc. Roy. Soc. London, 207, pp. 187-217*

[8] R. Mehrotra and S. Nichani. "Corner Detection". *Pattern Recognition*. Vol. 23, No. 11, pp. 1223-1233, 1990.

[9] G. Olague and R. Mohr. "Optimal Camera Placement for Accurate Reconstruction", *Pattern Recognition* Vol. 35(4), pp. 927-944, April 2002.

[10] K. Rohr. "Recognizing Corners by Fitting Parametric Models". *International Journal of Computer Vision*. 9(3), pp. 213-230, Kluwer Academic Publishers, 1992.

[11] P. L. Rosin. "Augmenting Corner Descriptors". *Graphical Models and Image Processing*. Vol. 58, No. 3, May, pp. 286-294, 1996.

[12] Z. Zheng, H. Wang and E. K. Teoh. "Analysis of Gray Level Corner Detection". *Pattern Recognition Letters*, 20, pp. 149-162, Elsevier, 1999.